

## Exploiting Eye Colors for Better Iris Segmentation in Visible Wavelength Environments

Shaaban SAHMOUD 

*Fatih Sultan Mehmet Vakif University (FSMVU), Computer Engineering Department, İstanbul, Türkiye*

### Abstract

Iris segmentation is a crucial step in iris recognition systems. Iris segmentation in visible wavelength and unconstrained environments is more challenging than segmenting iris images in ideal environments. This paper proposes a new iris segmentation method that exploits the color of human eyes to segment the iris region more accurately. While most of the current iris segmentation methods ignore the color of the iris or deal with grayscale eye images directly, the proposed method takes benefits from iris color to simplify the iris segmentation step. In the first step, we estimate the expected iris center using Haar-like features. The iris color is detected and accordingly, a color-convenient segmentation algorithm is applied to find the iris region. Dealing separately with each iris color set significantly decreases the false segmentation errors and enhances the performance of the iris recognition system. The results of testing the proposed algorithm on the UBIRIS database demonstrate the robustness of our algorithm against different noise factors and non-ideal conditions.

**Keywords:** Iris Segmentation, Visible Wavelength Iris Images, Color-based Iris Segmentation, Eye Color Classification, Unconstrained Iris Recognition

### I. INTRODUCTION

With the increasing attention to iris biometrics, the need for an accurate and fast recognition system has increased [1]. The human iris has many features which make it a highly reliable biometric. Examples of these features are the constancy of iris patterns over the years, the high complexity and randomness patterns, and the exceptional amount of entropy, enabling the avoidance of false match and false reject errors [2]. As a result, iris recognition has a wide use range from border authentication systems [3], to forensics applications [4], to ATM systems [5].

A classical iris recognition system commonly consists of four main steps: iris region segmentation, iris region normalization, features encoding from the normalized iris image, and iris code matching [6]. The first step (iris region segmentation) is considered the most critical of these four steps. In this stage, researchers confront numerous noise elements, especially within dynamic and non-ideal contexts. Moreover, making an error in this step by adding non-iris pixels to the real iris region or by removing some iris pixels from the real iris region, significantly affects/degrades the resulted iris template and consequently leads to false accept or false reject errors [7].

Iris recognition systems are categorized as constrained and unconstrained depending on the applicable circumstances. Some research mentions it as cooperative and non-cooperative [8]. When working with noisy iris images acquired in non-cooperative environments and under non-ideal imaging conditions, the iris identification methods proposed to deal with cooperative environments may not operate well. This is because iris images may include more difficult-to-separate noise factors in unconstrained environments that cannot be handled using traditional iris segmentation algorithms. Examples of such factors are specular reflections, luminance, high occlusions by eyelashes and eyelids, eyeglasses, and focusing problems. Fig. 1 gives two sample iris images. The first one was captured in visible wavelength and under an unconstrained environment, and the second image was captured in ideal conditions (constrained environment) with Near-infrared cameras (NIR).

In the iris segmentation step, the iris's inner and outer circular or uncircular boundaries are localized, and the regions that belong to other factors and cover or degrade the iris region should be removed. The upper and lower eyelashes, the eyelids, the eye pupil, and the iris regions that are affected by specular reflections are examples of these factors that should be detected and isolated from the iris region [13]. In the second step, the segmented iris

region is converted/normalized to a rectangular region to simplify the process of feature extraction. The third step called feature encoding or feature extraction is carried out on the segmented and normalized iris region by applying a convenient filter or feature extraction technique to produce the first version of the iris biometric template. Normally, the output of this step is two identical size arrays called iris template/code and iris mask. The iris code represents the unique features of the considered person, and the mask array is used to enhance the hamming distance results by excluding the non-iris pixels. In the fourth and last step, the extracted iris code is compared with one (verification) or more (identification) different iris codes to determine if they belong to the same person or not. The comparing process is usually done by calculating the Hamming Distance (HD) between the two compared iris codes [15]. Of the four steps of iris recognition, the second step which is iris segmentation is the hardest and most studied step in literature. This is because this step processes directly the noisy iris image that may be affected by many real-world noise sources and dynamic environments. Moreover, all other iris recognition steps rely on its result. Consequently, if any error occurs in the segmentation step, it will directly affect the feature extraction step and cause degradation in the iris code [14].

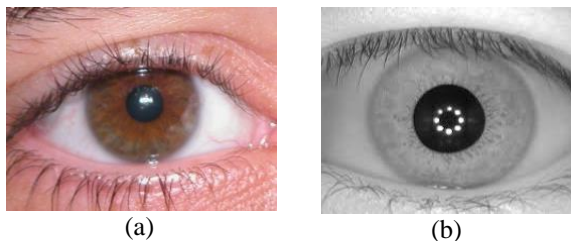


**Figure 1:** Two iris images. (a) from the UBIRIS database, and (b) from the CASIA database.

Since the first automated iris recognition was proposed in 1997 [7], many algorithms have been developed in this field where most of them focus on cooperative systems under controlled conditions. Recently, there has been increasing research attention to non-cooperative and unconstrained iris recognition systems that can work in non-ideal conditions. By reviewing the related work in iris recognition, we noted that most of the current iris segmentation methods ignore the color of the iris and prefer to deal with grayscale eye images directly [9,10,11]. Our main motivation in this work is that many false iris segmentation cases occur due to the wide color ranges of human iris regions and trying to deal with these heterogeneous colored irises using one methodology. Based on these observations, a new fast segmentation method that utilizes the iris color to boost the robustness and efficiency of the iris segmentation step is proposed. We believe that exploiting the color of the iris can significantly contribute to enhancing and simplifying the segmentation step, especially in

unconstrained environments. The main contributions of this study are summarized as follows:

1. A novel color-based iris segmentation algorithm for images captured in unconstrained environments is proposed. It first detects the color of the iris/eye and then deals with each eye class independently using different parameters.
2. A fast new method to estimate the pupil and iris centers using a Haar-like feature is proposed. It can quickly and efficiently search for the candidate center of the iris and significantly reduces the region of interest for the next steps in the segmentation process.
3. A new method to detect the color of the iris is proposed using the K-means clustering algorithm.
4. More convenient methods for unconstrained environments to find and isolate non-iris regions such as eyelashes, eyelids, and specular reflections are proposed and utilized.

To the best of our knowledge, this paper is the first research that detects the iris color and utilizes it in the iris segmentation step. Our experimental results confirm the significance of classifying irises based on their colors where it enables the detection of complex and challenging noise regions that cannot be detected by most of the existing segmentation methods.

This paper is organized as follows: Section 2 provides a brief overview of research on iris segmentation in unconstrained environments. A detailed description of the proposed color-based segmentation method is given in Section 3. In Section 4, we present and discuss the results of our experimental study. Section 5 concludes the paper and gives some future work directions.

## II. RELATED WORK

This section provides a brief overview of the literature on iris segmentation in unconstrained and non-cooperative environments. Over the past two decades, many algorithms have been proposed to deal with iris segmentation in non-ideal environments where most of which are developed by enhancing the traditional iris segmentation algorithms or adding more pre-processing steps before segmentation starts. Segmentation methods can be classified into many categories using different criteria such as if the model is boundary-based or pixel-based [9] if the model starts by searching for iris, pupil, or sclera [10], and depending on the primary segmentation operator or approach [10].

One of the first methods used in iris segmentation is the integrodifferential operator. It was proposed by Daugman in his fully proposed iris recognition system [11]. This operator obtains excellent results in ideal conditions where its performance significantly degrades in noisy environments. In [12], the authors proposed an enhancement version of the integrodifferential operator of the former model to perform more efficiently in unconstrained environments. A multi-step clustering-based

segmentation mechanism was proposed in [13] to obtain better results in noisy environments. In [14], the Hough transform was combined with the integrodifferential operator to overcome the problems of both methods and achieve better results. The authors in [15] focused on minimizing the execution time of the integrodifferential operator by utilizing the average square shrinking method.

Circular Hough Transform (CHT) is one of the most popular methods used in iris segmentation in noisy environments [16]. Usually, it is used after applying a suitable edge detection method. Although CHT performs very well in unconstrained environments, it does have a high computational cost and assumes that the iris is circular [17]. In literature, many researchers have been working to address these two problems [18-20] using several approaches. One technique is to reduce the search region of the iris to decrease the computational time of CHT [10]. One problem with this model is dealing with the off-angle scenarios that generate uncircular iris borders. In another interesting research [42], the authors used a new color segmentation method to exclude the affected regions by visible light from the iris region. After that, the iris and pupil are localized by applying two circular edge detection.

To deal with the uncircular borders of the iris, the active contour is a common technique proposed to segment iris regions. For example, in [21], the outer and inner boundaries of the iris are estimated using a technique called geodesic active contours. In another work [22], an adaptive iris segmentation method was proposed using an updated geodesic active contours model. In literature, many other iris segmentation methods were presented by using different versions of the active contours model [23], [24]. The main problem of active contours algorithms is the high sensitivity to noise which reduces their performance in unconstrained environments.

As with many other image processing and computer vision applications, deep learning and Convolutional Neural Networks (CNNs) [25, 39, 40, 41, 43, 44] have been effectively used in the iris segmentation step. IrisParseNet [26] is one of the first attempts to propose a deep learning-based framework to solve the iris segmentation problem. The correlations between the iris, sclera, and pupil were utilized to boost the iris segmentation process. In [27], the authors proposed a general deep learning method for all steps of iris recognition (including iris segmentation) by designing a fully convolutional neural network. The DeepIrisNet [28] is another deep learning-based model that uses highly deep architecture to detect the iris region accurately.

As discussed in the previous section, all the current iris segmentation methods deal with all types and classes of the iris using one methodology which causes many errors in the segmentation step because of the wide possible color ranges of the human iris. At the same time, most of the proposed iris segmentation

methods require a long execution time, which makes it slows down the execution in real-time scenarios.

### III. PROPOSED METHODOLOGY

This section describes the steps of our proposed color-based segmentation algorithm. As described in Section 2, common iris segmentation methodologies are designed to either deal with grayscale iris images directly or convert the colored iris image to grayscale image first then apply the remaining segmentation steps. In both situations, the color of the iris is ignored, and no more benefits are gained from the different available color spaces. One of the most common sources of segmentation errors is the high color variations of human irises. Most of the current iris segmentation algorithms that deal with unconstrained iris images are designed to work for normal and common human irises and they face some difficulties when dealing with very high or very low color intensities in the iris region. Figure 2 shows two samples of iris images from the UBIRIS v1 database [32] that have a high difference in color information. In dark color iris, it becomes very difficult to determine and remove the dark color noise factors such as pupil and eyelashes, whereas in light color iris, it is difficult to detect and remove specular reflections that may occur in a visible wavelength environment.

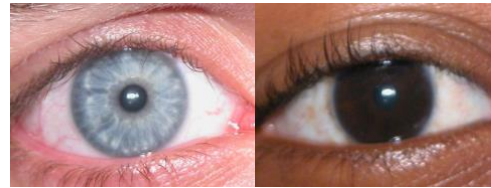


**Figure 2:** Two sample iris images from the UBIRIS v1 database with light and dark colors.

The proposed segmentation algorithm is designed to exploit the color information of the iris to achieve more robust and accurate segmentation with low execution time. The segmentation process begins with the estimation and detection of the color of the eye or iris, and then different segmentation and noise removal techniques are applied according to the detected iris color. Figure 3 shows the block diagram of the proposed segmentation algorithm.

The essential point consists of determining the iris color and dealing with each iris color/type more specifically to accurately find the iris region pixels and remove the non-iris pixels. The process starts by searching for the expected iris region in the image then; the pupil of the eye is localized by applying the circular Hough transform on the output image of the previous step. Estimating the expected iris region is an essential step to eliminate a large portion of non-iris regions which helps in avoiding errors that occur in non-iris regions as well as reducing the searching time

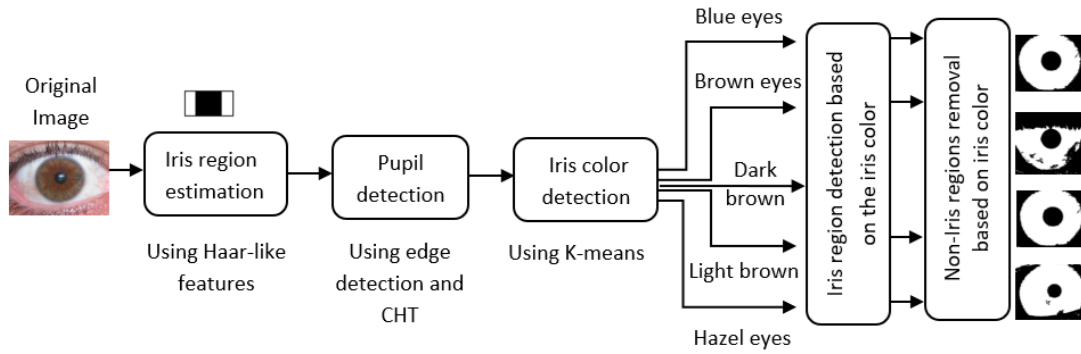


**Figure 3:** The block diagram of the proposed color-based iris segmentation algorithm.

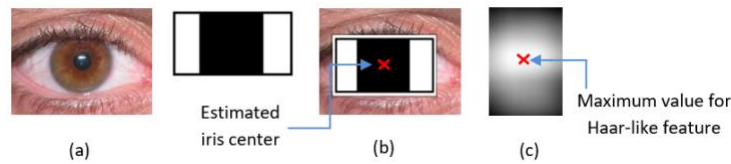


**Figure 4:** The selected Haar-like feature to estimate the iris center.

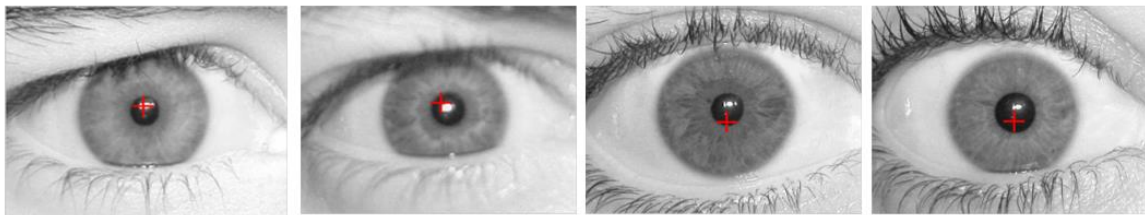


**Figure 5:** Determine the estimated iris centers for four sample images using our proposed Haar-like feature method.

of the next steps. After removing the pupil region, the color of the iris is detected using the k-means algorithm. Based on the color of the iris, several color-specific techniques are applied to accurately classify iris pixels and remove the non-iris regions. The color-specific techniques enable higher accuracy of pixel classification and eliminate the noise sources with minimal computations. In the following subsections, we explain the steps of the proposed algorithm in detail.

### 3.1 Iris Region Estimation

Searching for the iris region can face two types of errors which are errors inside the iris region (such as pupil, luminance, and eyelashes), and errors outside the iris region (such as eyelashes, eyebrows, and glass frame). Dealing directly with the entire eye image exposes the segmentation algorithm to both error types. Therefore, many segmentation algorithms employ different pre-segmentation methods to delete the skin and sclera regions such as the k-means algorithm and thresholding techniques [10] [29]. In

this paper, a new method inspired by Haar-like features is proposed to quickly search for the expected iris center [30]. Haar-like features are widely used in many object recognition algorithms such as the well-known Viola-Jones face detection algorithm. The key advantage of Haar-like features over other techniques is its low computational cost since it can be calculated in constant time regardless of the used feature size. To find the estimated center of the iris, a Haar-like feature is applied to the iris image as shown in Fig. 4. The selected feature measures the difference in intensity between the iris region and regions around the iris from the two sides. This feature is selected based on observing that the iris region is often darker than its two sides which usually represent the sclera region. Another advantage of using this feature is that it is relatively insensitive to iris size and iris location.

The Haar-like feature is moved over the input iris image, and it is calculated by subtracting the sum of the pixels that lie within the white rectangles from the sum of pixels in the black rectangle. We assume that



**Figure 6:** One sample iris image from each type of the five considered color classes.

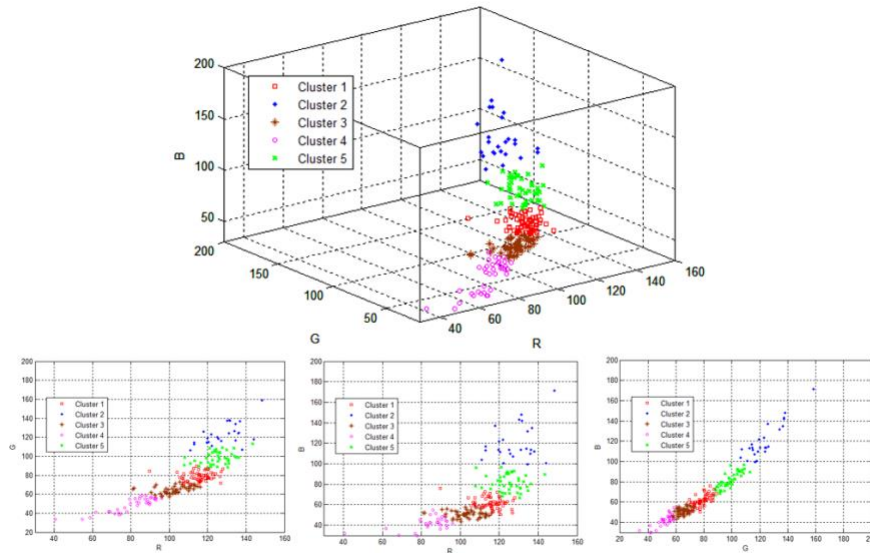


**Figure 7:** Distribution of the colors of iris images in the RGB color space. Clusters 1, 2, 3, 4, and 5 represent the light brown, blue, brown, dark brown, and hazel irises.

the location where the Haar-like feature obtains the maximum value represents the expected iris center. Figure 4.c shows the resulting image after applying this step on a sample iris image. As expected, the feature obtains small values in the image edges and large values around the center of the image while moving over the iris. Note that this step is used to only decrease the search space for the next steps and the obtained iris center may not be exactly the real iris center. Figure 5 shows the detected iris center of some sample images from the UBIRIS database.

### 3.2. Pupil Region Isolation

Detecting and removing the pupil region in non-cooperative environments is not a simple task as in controlled environments. This is because of the low contrast between the color intensities of the pupil region and the iris region, mostly in dark-colored eyes (see Fig. 3). Therefore, removing the pupil region in those environments needs more effort and specific handling. To address this issue, we used our previously proposed pupil isolating method [10], [6], which primarily employs the Canny edge detection and the circular Hough transform. This method is characterized by its high speed and low influence on other error factors in unconstrained environments. The following steps summarize this method: The iris image is enhanced by applying image-adjusting

techniques to increase the contrast between the iris and pupil regions.

1. The pupil searching area is minimized by restricting the search region to only a small square. The center of this square is equal to the expected iris center obtained from the previous step.
2. The Canny edge detection is applied [31] to obtain the binary edge image.
3. The circular Hough transform is applied to localize the pupil region.

### 3.3. Iris Color Detection

Detecting the iris color is a crucial step of our proposed segmentation algorithm since the remaining steps will be significantly affected by the obtained result from this step. By analyzing the iris images of the UBIRIS v1 database [32], we classified irises into five classes according to their colors. In the real world, there are more than five iris color types, but since our experimental results are conducted using the UBIRIS database only five iris colors are considered. The five classified colors are blue, mixed blue/green, and red (hazel), light brown, brown, and dark brown.

Fig. 6 shows one sample image from each of the five color classes. As seen in the figure, the blue irises have the highest intensity values since they are closer to the white color. Hazel irises usually consist of two colors as described in the previous section. The other

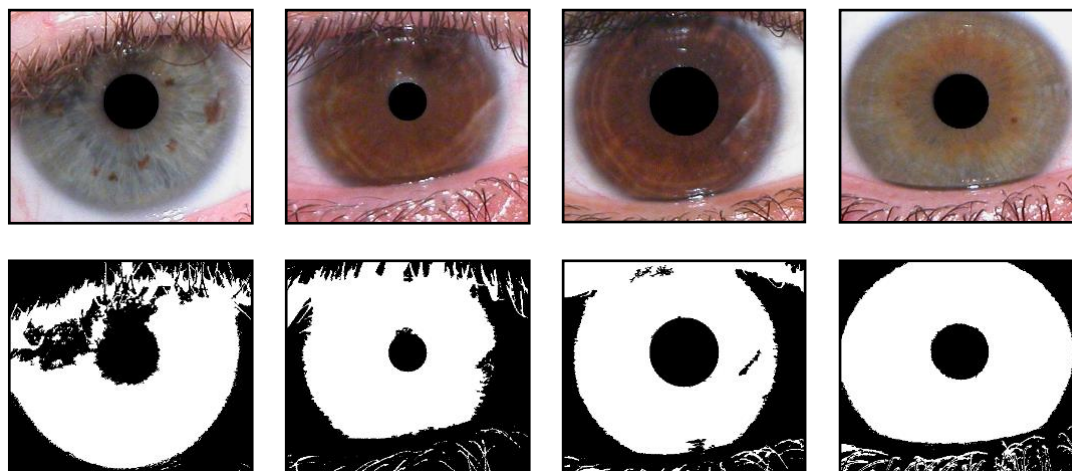


**Figure 8:** Segmented iris images using the proposed color-based algorithm.

three iris types in the UBIRIS database are the three different levels of brown color. We divided them into three types since the intensity difference between them is very high. To understand the overall perspective of iris colors, we experimented to view the average color of each iris image in the UBIRIS v1 database. The 241 considered iris pictures for 241 persons are selected from the UBIRIS v1 database [32]. The irises are manually segmented, and all non-iris regions are removed, then we computed the average intensity of each iris for the three-color components of RGB color space which are red, green, and blue. After that, the iris images are classified into five clusters using the K-mean algorithm. Fig. 7 shows the distribution of iris image colors in the RGB color space.

By examining Figure 7, we can see that there is a wide variation in the color intensity levels of the considered irises. Intuitively, dealing with each color level separately in the segmentation process is much better than dealing with all these high ranges of colors as one class. Furthermore, dealing with each class differently enables us to solve the problems of each class without affecting on results of other classes which addresses the shortcomings of many existing segmentation algorithms. It is important here to remember that the proposed algorithm is scalable which means that we can simply extend it to be able to handle other types of irises such as green, red, and violet irises.

**Table 1** Low and high threshold values for the five considered color classes.

| Color    |   | Light brown | Brown | Dark brown | Blue | Hazel |
|----------|---|-------------|-------|------------|------|-------|
| <b>R</b> | L | 75          | 52    | 5          | 85   | 80    |
|          | H | 150         | 140   | 74         | 175  | 170   |
| <b>G</b> | L | 43          | 30    | 4          | 80   | 55    |
|          | H | 120         | 95    | 65         | 178  | 143   |
| <b>B</b> | L | 22          | 20    | 1          | 65   | 35    |
|          | H | 115         | 95    | 48         | 195  | 140   |

### 3.4. Iris Region Localization

Our iris region segmentation uses the RGB three color components to accurately characterize the pixels of the iris region from the other eye and noise pixels. For each color component, we calculated the minimum and maximum thresholds that can characterize the five different color classes. The limits of each color component are calculated by performing a preliminary experiment using the method presented in [5]. The difference in our proposed algorithm is that we estimate the minimum and maximum thresholds for each color class separately. To do this, a total of 241 iris images for different 241 human eyes are used. By addressing each color independently, the algorithm becomes able to precisely find the iris pixels and exclude the non-iris pixels without struggling with the segmentation issues that appear in other segmentation algorithms [29]. The irises are manually segmented, and all non-iris regions are removed, then we computed the histogram of intensities for each color class using the three-color components of RGB color space. The thresholds are computed using  $1.5\alpha$ , such that  $\alpha$  denotes the standard deviation of the intensity's histogram for each color component. The lower and upper thresholds of each color class are given in Table 1. A pixel is classified as an iris pixel if its red, green, and blue intensity values fall within the range determined by the minimum and maximum thresholds of each color component for this color class.

The results of applying this step on a sample set of iris images obtained from the previous step are shown in Figure 8. By examining the segmented images in this figure, it is noted that the proposed segmentation algorithm can efficiently find and recognize iris pixels from different color levels and accurately isolate the sclera, eyelashes, and specular reflection pixels. Although the proposed algorithm can isolate most of the non-iris and noise regions without any extra effort, there are still small regions that require to be removed in some situations such as lower and upper eyelashes. These situations occur normally when the iris color is

dark as in brown and dark brown images where it becomes more difficult to separate the small regions of eyelashes from the iris region. For that reason, another step of noise cleaning is required to completely remove all non-iris regions from the iris region.

### 3.5. Non-Iris Pixels Removal

As described in the previous step, for some dark irises, the upper and lower eyelashes still need handling to be completely removed. In unconstrained environments, determining and removing the eyelash regions that cover some parts of the iris is one of the most critical and hard tasks since it occurs very often. The proposed segmentation algorithm utilizes our previously proposed eyelash removal technique to delete the remaining non-iris pixels from the obtained image in the previous step [10]. This technique is especially proposed to robustly deal with eyelashes in unconstrained and visible wavelength environments, and as a result, it was applied in many other segmentation methods [29], [33]. The efficiency of this technique is due to the detection of eyelashes from the sclera region rather than the iris region as other algorithms do. Consequently, it can successfully isolate the eyelashes since the intensity difference between the sclera region and eyelashes region is very high and provides much better results than trying to isolate them from inside the iris region. The following steps summarize how the eyelash removal technique works:

1. Two rectangles in the sclera region are localized from the two sides of the iris region.
2. The horizontal Canny edge detection is applied on the two rectangle images to discover the edges between the sclera and eyelashes/eyelids, and then the resulting edge images are enhanced by morphological operations to delete the small noise points.
3. Locate the edge points on each side that represent eyelashes/eyelids and draw the arc that connects these two points to represent the eyelid location. To draw this arc its radius and center are calculated as explained in [4]. For the upper eyelid, all points after this arc are considered noise points that may belong to the upper eyelashes or eyelids.

In some rare cases, we get some blocks inside the iris region that are considered noise or non-iris regions where they are part of the iris region in real. To handle such cases, we conduct another adaptive process to correct the classification of these blocks by using again the iris color. This process simply checks if the considered iris has a dark or light color. If it has a dark color like brown or dark brown and these blocks have large intensity values, then these blocks are considered specular reflections. Conversely, if the iris has a light color like the blue and these blocks have large intensity values, then these blocks are considered as parts of the iris region.

## IV. RESULTS AND DISCUSSION

In this section, we give a brief description of the UBIRIS database that we used to test our segmentation algorithm, and then present the obtained results of comparing our color-based segmentation algorithm with other methodologies.

### 4.1. UBIRIS iris database

The UBIRIS [32] database is one of the most popular databases for iris recognition in visible wavelength and unconstrained environments. It is a publicly available database with 1877 images taken from 241 persons. It simulates the unconstrained imaging conditions by providing different types of noise factors such as eyelid and eyelash iris obstruction, specular reflections, contrast, and different focus levels. The images of UBIRIS can be classified into different classes based on three parameters focus, reflections, and the visibility of the iris using three scale levels which are good, average, and bad. To investigate the performance of our algorithm, we considered all the 1877 images of the UBIRIS v1 database that have 800/600 resolution. Figure 1 and Figure 6 give some examples of the images of this database. As shown from these figures, UBIRIS v1 includes a diverse set of irises with different features and colors which makes it suitable for training and testing our proposed algorithm.

### 4.2. Results

The proposed segmentation algorithm is implemented using MATLAB software. As we described in the previous section, the iris region is estimated first using Haar-like features then the pupil is localized and removed. After that, the color of the iris is detected using the k-means algorithm, and accordingly, a set of different thresholding techniques are applied to determine the pixels of each iris type. Finally, a set of robust techniques is conducted to clean the remaining non-iris pixels.

Figure 9 shows a sample of segmented iris images after applying our iris segmentation algorithm. The first row represents the original iris images; the second row shows the images after removing the pupil and upper eyelids regions and marking them with black pixels. In the third row of the figure, we give the binary images after detecting the color of the iris and classify its pixels accordingly. The segmented images confirm the high efficiency of our proposed methodology in both determining the iris regions and isolating the noise regions especially those that occur as a result of specular reflections and upper eyelashes. While our algorithm can accurately isolate the specular reflection regions, many proposed segmentation algorithms fail or face some difficulties in dealing with such challenging tasks especially when

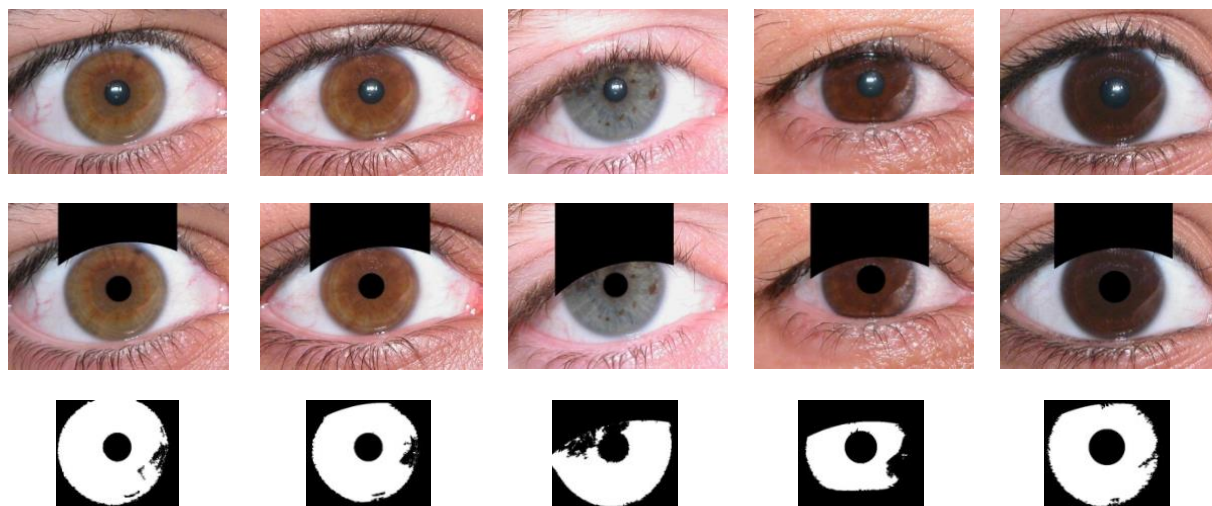


**Figure 9:** A sample set of segmented irises using the proposed color-based algorithm where the third row represents the binary image of the segmented iris region.

**Table 2:** Performance summary of the proposed segmentation algorithm concerning other methods.

| Method                | Tested Images | Iris (%) | Pupil (%) | Eyelashes and eyelids (%) | Time (s) |
|-----------------------|---------------|----------|-----------|---------------------------|----------|
| Daugman [10]          | UBIRIS v1     | 95.22    | 95.22     | -                         | 3.20     |
| Wildes [14]           | UBIRIS v1     | 98.60    | 96.60     | 95.32                     | 2.31     |
| Sahmoud et al. [4]    | UBIRIS v1     | 98.12    | 96.52     | 96.12                     | 1.90     |
| Fast Multi-Models [5] | 600           | 96.75    | 96.25     | 96.75                     | 1.12     |
| Fourier spectral [35] | UBIRIS v1     | 98.49    | 94.47     | -                         | -        |
| Proposed Algorithm    | UBIRIS v1     | 98.92    | 98.01     | 98.76                     | 1.64     |

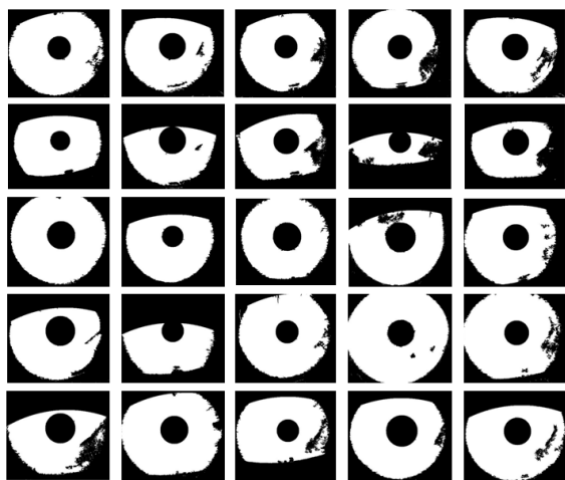
working under visible wavelength environments. The results show that our algorithm can detect all types of specular reflections and shadows that most other algorithms fail to detect. We found that even in the binary truth table images that are used in testing the performance of segmentation methods or training the models to deal with iris segmentation, there are some undetected regions for shadow and specular reflections that our proposed algorithm can detect.

Table 2 summarizes the results of our comparative study to investigate the segmentation performance between the proposed algorithm and other previously proposed algorithms. To assess the performance of algorithms in detail, four performance metrics are considered to measure the efficiency of algorithms, iris segmentation accuracy, pupil isolation accuracy, eyelashes and eyelids isolation accuracy, and average execution time in seconds. For the iris, pupil, and eyelashes the accuracy is obtained by visual inspection of each iris image as done in [10], [35]. A correct segmentation is considered when the detected iris, pupil, and eyelid borders fall exactly into the real borders of these objects. While some researchers use the ground truth of manually segmented iris images to

compare their proposed segmentation algorithms, we prefer not to use it for two reasons. First, there is no full ground truth available for the UBIRIS v1 database and second, most of the available ground truth binary images ignore some noise factors such as specular reflections and shadows which causes unfair comparison. The average segmentation time is obtained by considering the mean processing time of 100 iris images. All the algorithms except the Fourier spectral algorithm were implemented and tested in Matlab where implementations are not perfectly optimized for fast execution speed. Since there is no available public code for the Fourier spectral method, we report the result presented in [34].

From the results of Table 2, it is observed that the proposed segmentation algorithm performs better than most of the other compared algorithms even in the presence of noise factors under non-ideal conditions. It obtained the best segmentation accuracy in the pupil, eyelashes, and eyelids, the second-best results regarding time, and the third-best results for the iris. Wildes’ method [7] achieved the best results with a slightly better result than the proposed algorithm, but it faces some difficulties in dealing with eyelashes and

pupil regions where its performance decreases to 95.3 and 96.6 respectively. Moreover, it spends 40% more time on average than the proposed algorithm. On the other hand, Daugman's algorithm [3] which was originally developed for cooperative environments was significantly affected by existing noise factors in the UBIRIS database and obtained around 4.8% percentage of false segmentation. One reason for this is the low image quality of noisy images which is considered insufficient for the integrodifferential operator to work efficiently. Sahnoud et al. [10] algorithm performs well in iris and pupil segmentation, but it is observed that it fails in some complex eyelashes and shadow situations. Moreover, both Sahnoud et al. [10] algorithm and Wildes' [7] algorithm assume that the iris is circular which causes some inaccurate results in the off-angle iris images. The fast multi-model method [29] needs both training and testing sets; therefore, we tested it under 600 images only. It achieved acceptable results, but it is still not as good as other algorithms since it concentrates on execution speed more than segmentation accuracy. For mPA metrics results, our proposed algorithm obtained the second-best results whereas the DFCN algorithm achieved the best results. One reason for this is the high efficiency of the



deep learning approach used in DFCN which is one of our future work points.

**Figure 10:** A sample set of binary images that represent the segmented irises using the proposed color-based algorithm.

Note that the iris color can be also important in soft biometrics where the color and the size of the eye are included in the features for human identification and verification processes. Fig. 10 shows the binary images for a set of segmented irises using the proposed color-based algorithm. The binary images clearly demonstrate the ability of the proposed

algorithm to deal with different levels of eyelids and eyelash occlusions. Furthermore, the specular reflections and shadows are accurately isolated from the iris regions. According to our results, most UBIRIS iris images are exposed to specular reflections from the right sides of the irises more than the left sides.

Regarding the execution time of the compared algorithms, we observed that the fast multi-models method [29] is the fastest. This result is reasonable since it utilizes a multi-thresholding mechanism to detect iris pixels in different color spaces. The proposed method's computation time is the second-best one followed by Sahnoud et al. method. Note that the implementation of these algorithms is not optimized well to have low computation time, we believe that with more code optimization and by implementing our method using C++ the computation time can be significantly enhanced. On the other hand, the proposed algorithm sometimes fails in segmenting iris images in special cases. Fig. 11 shows some examples of failed or non-accurate classified iris images. The main issue of the proposed algorithm is when we have two high and low-intensity colors in the same iris as shown in Fig. 11. In this case, the proposed algorithm may exclude some iris regions and consider them as specular reflections or noise. In addition, our algorithm may face some difficulties when handling images of individuals with glasses especially when the glasses frame includes diverse colors that interfere with the iris colors.

The high speed of the proposed algorithm compared to other algorithms enables it to be used efficiently in real-time or online applications without affecting the segmentation efficiency. Dealing with each iris color level separately can enhance the segmentation results (as shown in Table 2) and reduce the iris regions that are excluded falsely during noise-cleaning techniques. Moreover, the proposed algorithm can be used as a first processing step for other medical or eye-tracking algorithms.

## V. CONCLUSION

In this paper, we proposed a new robust iris segmentation algorithm that utilizes the color information of human eyes to enhance the iris segmentation step in unconstrained and non-cooperative environments. While most of the current iris segmentation methods ignore the iris color, the proposed algorithm benefits from it and uses it to deal with each color separately more specifically during segmentation. In the first step, the expected iris center is estimated using Haar-like features, and then the iris

color is detected by using k-means clustering. Accordingly, a color-convenient segmentation algorithm is applied to classify the pixels of the candidate region into iris and non-iris pixels. To remove the other noise factors such as eyelids, eyelashes, luminance, and shadows, several robust noise removal techniques are applied. Our experimental results on the UBIRIS database demonstrated the robustness of our algorithm against different noise factors and non-ideal conditions. Moreover, the results prove the efficiency of dealing with each iris color set separately which significantly decreases the false segmentation errors and enhances the performance of the iris recognition system. The results confirmed the efficiency of the proposed approach compared to other state-of-the-art algorithms from different approaches. In addition, the proposed algorithm showed promising results regarding the execution time since the results showed that the proposed method is faster than other approaches by 23% on average while still obtaining competitive accuracy results.

In future work, we are planning to extend our work by including other iris colors that do not exist in the UBIRIS database such as green and red iris colors. In addition, optimizing the code of our algorithm and merging it with current CNN algorithms is another planned research work [38].

## REFERENCES

- [1] Kak, N., Gupta, R., & Mahajan, S. (2010). Iris recognition system. *International Journal of Advanced Computer Science and Applications*, 1(1), 34-40.
- [2] Daugman, J. (2001). Statistical richness of visual phase information: update on recognizing persons by iris patterns. *International Journal of computer vision*, 45(1), 25-38.
- [3] Daugman, J. (2004). Iris recognition border-crossing system in the UAE. *International Airport Review*, 8(2).
- [4] Chen, J., Shen, F., Chen, D. Z., & Flynn, P. J. (2016). Iris recognition based on human-interpretable features. *IEEE Transactions on Information Forensics and Security*, 11(7), 1476-1485.
- [5] Thepade, D. S., & Mandal, P. R. (2014). Novel iris recognition technique using fractional energies of transformed iris images using haar and kekre transforms. *International Journal of Scientific & Engineering Research*, 5(4).
- [6] Sahnoud, S. A. I. (2011). Enhancing iris recognition.
- [7] Wildes, R. P. (1997). Iris recognition: an emerging biometric technology. *Proceedings of the IEEE*, 85(9), 1348-1363.
- [8] Bowyer, K. W., Hollingsworth, K. P., & Flynn, P. J. (2013). A survey of iris biometrics research: 2008–2010. In *Handbook of iris recognition* (pp. 15-54). Springer, London.
- [9] Liu, N., Li, H., Zhang, M., Liu, J., Sun, Z., & Tan, T. (2016). Accurate iris segmentation in non-cooperative environments using fully convolutional networks. In *2016 International Conference on Biometrics (ICB)* (pp. 1-8). IEEE.
- [10] Sahnoud, S. A., & Abuhaiba, I. S. (2013). Efficient iris segmentation method in unconstrained environments. *Pattern Recognition*, 46(12), 3174-3185.
- [11] Daugman, J. (2009). How iris recognition works. In *The Essential Guide to Image Processing* (pp. 715-739). Academic Press.
- [12] Tan, T., He, Z., & Sun, Z. (2010). Efficient and robust segmentation of noisy iris images for non-cooperative iris recognition. *Image and vision computing*, 28(2), 223-230.
- [13] Proença, H., & Alexandre, L. A. (2007). The nice. i: noisy iris challenge evaluation-part i. In *2007 First IEEE International Conference on Biometrics: Theory, Applications, and Systems* (pp. 1-4). IEEE.
- [14] Tisse, C. L., Martin, L., Torres, L., & Robert, M. (2002). Person identification technique using human iris recognition. In *Proc. Vision Interface* (Vol. 294, No. 299, pp. 294-299).
- [15] Shamsi, M., Saad, P. B., Ibrahim, S. B., & Kenari, A. R. (2009). Fast algorithm for iris localization using Daugman circular integro differential operator. In *2009 International Conference of Soft Computing and Pattern Recognition* (pp. 393-398). IEEE.
- [16] Pedersen, S. J. K. (2007). Circular hough transform. *Aalborg University, Vision, Graphics, and Interactive Systems*, 123(6).
- [17] Uhl, A., & Wild, P. (2012). Weighted adaptive hough and ellipsopolar transforms for real-time iris segmentation. In *2012 5th IAPR international conference on biometrics (ICB)* (pp. 283-290). IEEE.
- [18] Huang, J., Wang, Y., Tan, T., & Cui, J. (2004, August). A new iris segmentation method for recognition. In *Proceedings of the 17th International Conference on Pattern Recognition, 2004. ICPR 2004.* (Vol. 3, pp. 554-557). IEEE.
- [19] Kong, W. K., & Zhang, D. (2001). Accurate iris segmentation based on novel reflection and eyelash detection model. In *Proceedings of 2001 International Symposium on Intelligent Multimedia, Video and Speech Processing. ISIMP 2001* (IEEE Cat. No. 01EX489) (pp. 263-266). IEEE.
- [20] Ma, L., Wang, Y., & Tan, T. (2002). Iris recognition using circular symmetric filters. In *Object recognition supported by user interaction for service robots* (Vol. 2, pp. 414-417). IEEE.

- [21] Banerjee, S., & Mery, D. (2015). Iris segmentation using geodesic active contours and grabcut. In *Image and Video Technology* (pp. 48-60). Springer, Cham.
- [22] Shah, S., & Ross, A. (2009). Iris segmentation using geodesic active contours. *IEEE Transactions on Information Forensics and Security*, 4(4), 824-836.
- [23] Ouabida, E., Essadique, A., & Bouzid, A. (2017). Vander Lugt Correlator based active contours for iris segmentation and tracking. *Expert Systems with Applications*, 71, 383-395.
- [24] Ross, A., & Shah, S. (2006). Segmenting non-ideal irises using geodesic active contours. In *2006 Biometrics Symposium: Special Session on Research at the Biometric Consortium Conference* (pp. 1-6). IEEE.
- [25] Badrinarayanan, V., Kendall, A., & SegNet, R. C. (2015). A deep convolutional encoder-decoder architecture for image segmentation. *arXiv preprint arXiv:1511.00561*, 5.
- [26] Wang, C., Zhu, Y., Liu, Y., He, R., & Sun, Z. (2019). Joint iris segmentation and localization using deep multi-task learning framework. *arXiv preprint arXiv:1901.11195*.
- [27] Zhao, Z., & Kumar, A. (2017). Towards more accurate iris recognition using deeply learned spatially corresponding features. In *Proceedings of the IEEE international conference on computer vision* (pp. 3809-3818).
- [28] Gangwar, A., & Joshi, A. (2016). DeepIrisNet: Deep iris representation with applications in iris recognition and cross-sensor iris recognition. In *2016 IEEE international conference on image processing (ICIP)* (pp. 2301-2305). IEEE.
- [29] Sahnoud, S., & Fathee, H. N. (2020). Fast Iris Segmentation Algorithm for Visible Wavelength Images Based on Multi-color Space. In *International Conference on Advanced Concepts for Intelligent Vision Systems* (pp. 239-250). Springer, Cham.
- [30] Viola, P., & Jones, M. (2001). Rapid object detection using a boosted cascade of simple features. In *Proceedings of the 2001 IEEE computer society conference on computer vision and pattern recognition. CVPR 2001* (Vol. 1, pp. I-I). Ieee.
- [31] Bao, P., Zhang, L., & Wu, X. (2005). Canny edge detection enhancement by scale multiplication. *IEEE transactions on pattern analysis and machine intelligence*, 27(9), 1485-1490.
- [32] Proença, H., & Alexandre, L. A. (2005). UBIRIS: A noisy iris image database. In *International Conference on Image Analysis and Processing* (pp. 970-977). Springer, Berlin, Heidelberg.
- [33] Gragnaniello, D., Poggi, G., Sansone, C., & Verdoliva, L. (2014, November). Contact lens detection and classification in iris images through scale invariant descriptor. In *2014 Tenth International Conference on Signal-Image Technology and Internet-Based Systems* (pp. 560-565). IEEE.
- [34] Puhan, N. B., Sudha, N., & Sivaraman Kaushalram, A. (2011). Efficient segmentation technique for noisy frontal view iris images using Fourier spectral density. *Signal, Image and Video Processing*, 5(1), 105-119.
- [35] Proença, H., & Alexandre, L. A. (2006). Iris segmentation methodology for non-cooperative recognition. *IEE Proceedings-Vision, Image and Signal Processing*, 153(2), 199-205.
- [36] Bazrafkan S, Thavalengal S, Corcoran P. (2018). An end-to-end deep neural network for iris segmentation in unconstrained scenarios. *Neural Networks*. 106:79-95.
- [37] Chen Y, Wang W, Zeng Z, Wang Y. (2019). An adaptive CNNs technology for robust iris segmentation. *IEEE Access*. 7:64517-64532
- [38] Fathee, H., & Sahnoud, S. (2021). Iris segmentation in uncooperative and unconstrained environments: State-of-the-art, datasets and future research directions. *Digital Signal Processing*, 118, 103244.
- [39] Li, Xi, Tian Li, Shaoyi Li, Bin Tian, Jianping Ju, Tingting Liu, and Hai Liu. (2023). "Learning fusion feature representation for garbage image classification model in human-robot interaction." *Infrared Physics & Technology* 128: 104457.
- [40] Liu, Tingting, Jixin Wang, Bing Yang, and Xuan Wang. (2021). "NGDNet: Nonuniform Gaussian-label distribution learning for infrared head pose estimation and on-task behavior understanding in the classroom." *Neurocomputing* 436: 210-220.
- [41] Liu, Tingting, Bing Yang, Hai Liu, Jianping Ju, Jianyin Tang, Sriram Subramanian, and Zhaoli Zhang. (2022). "GMDL: Toward precise head pose estimation via Gaussian mixed distribution learning for students' attention understanding." *Infrared Physics & Technology* 122 (2022): 104099.
- [42] Jeong, D.S., Hwang, J.W., Kang, B.J., Park, K.R., Won, C.S., Park, D.K. and Kim, J., (2010). A new iris segmentation method for non-ideal iris images. *Image and vision computing*, 28(2), pp.254-260.
- [43] Toizumi, Takahiro, Koichi Takahashi, and Masato Tsukada. (2023). "Segmentation-free direct iris localization networks." In *Proceedings of the IEEE/CVF Winter Conference on Applications of Computer Vision*, pp. 991-1000.
- [44] Chen, Ying, Huimin Gan, Huiling Chen, Yugang Zeng, Liang Xu, Ali Asghar Heidari, Xiaodong Zhu, and Yuanning Liu. (2023) "Accurate iris segmentation and recognition using an end-to-end unified framework based on MADNet and DSANet." *Neurocomputing* 517: 264-278.